European Journal of Pharmaceutics and Biopharmaceutics 123 (2018) 84–94

Contents lists available at ScienceDirect

European Journal of Pharmaceutics and Biopharmaceutics

journal homepage: www.elsevier.com/locate/ejpb

Research paper

Retrograded starch/pectin coated gellan gum-microparticles for oral administration of insulin: A technological platform for protection against enzymatic degradation and improvement of intestinal permeability

Andréia B. Meneguin[a,b,1], Eric Beyssac[c], Ghislain Garrait[c], Hassana Hsein[c], Beatriz S.F. Cury[a,*]

[a] Department of Drugs and Pharmaceuticals, School of Pharmaceutical Sciences, São Paulo State University-UNESP, 14800-903 Araraquara, SP, Brazil
[b] Interdisciplinary Laboratory of Advanced Materials, Centro de Ciências da Natureza – CNN, Universidade Federal do Piauí – UFPI, 64049-550 Teresina, PI, Brazil[1]
[c] Université Clermont Auvergne, INRA, UMR MEDIS, F-63000 Clermont-Ferrand, France

ARTICLE INFO

Keywords:
Insulin
Gellan gum
Retrograded starch
Colon-specific delivery
Microparticles

ABSTRACT

Gellan gum microparticles coated with colon-specific films based on retrograded starch and pectin was developed for enhancing the oral release of insulin (INS). The system developed promoted an impressive protection of INS (80%) after 120 min of incubation with trypsin and alpha-chymotrypsin, while only 3% of free INS remained intact after the same time, possibility due to the calcium chelating activity of the polymers in inhibiting the proteolytic activity. *In vitro* INS release in media simulating the gastrointestinal portions revealed a pH-dependent behavior, as well as the significance of the coating in lowering the release rates in relation to their counterparts. The permeability of INS on Caco-2 cells monolayers and excised rat intestine were significantly improved, mainly due to the influence of the anionic polymers on tight junctions opening, along with the excellent mucoadhesive properties of the gellan gum. All these features together contributed greatly to the hypoglycemic effect observed after the oral administration of the INS-loaded MP in diabetic rats, with reduction of up to 51% of blood glucose levels. The important findings of this work should contribute to the advances about the search of alternatives for oral administration of INS.

1. Introduction

After approval of recombinant insulin in 1982, the pharmaceutical industry has been revolutionized with the exponential increase of the therapeutic proteins approved by the FDA [1], which correspond to 50% of new drugs approved, reaching today about 200 new marketed biologics-based medicines [2]. The successful use of the biotherapeutics, mainly in the treatment of inflammatory, autoimmune, cardiovascular, metabolic diseases and in several types of cancer, is because of their numerous complex functions performed in the organism with greater specificity of action and safety over conventional chemical drugs, ensuring optimized therapeutic effects and reduced side effects [1,3].

It is worth watching that clinical efficacy of protein therapeutics is also a result of the pathway by which these biomolecules are administered, which in most cases occurs *via* parenteral route. A classic example of this is the treatment of diabetes mellitus (type-I and advanced cases of type-II), which over the decades has been carried out through daily subcutaneous injections of exogenous insulin (INS). Although the parenteral route of administration is quite effective in terms of bioavailability, the invasive routes cause several discomforts, including pain, local infection, lipoatrophy and psychological problems, reducing the compliance of the patient to the treatment [4,5].

In this regard, several strategies had been evaluated in order to find alternative routes for INS administration, such as the development of systems for nasal [6], rectal [7], pulmonary [8] and transdermal [9] routes. However, oral administration is considered the most convenient owing to its non-invasive nature, safety and comfort of the self-administration. In addition, INS is one of the few drugs benefited by the first hepatic bypass, *i.e.*, after its absorption by the intestinal epithelium, INS reaches the liver *via* the hepatic portal vein and inhibits directly the glucose production, mimicking the natural secretion of INS by islets of Langerhans. This effect cannot be reached by parenteral administration, as only 20% of the injected INS reaches the liver [10,11].

Unfortunately, the oral administration of proteins/peptides is limited by their intrinsic properties (high molecular weight, hydrophilic,

* Corresponding author.
E-mail addresses: abagliottim@hotmail.com (A.B. Meneguin), eric.beyssac@uca.fr (E. Beyssac), ghislain.garrait@uca.fr (G. Garrait), hassana_hsein@hotmail.com (H. Hsein), curybsf@fcfar.unesp.br (B.S.F. Cury).
[1] Present address.

https://doi.org/10.1016/j.ejpb.2017.11.012
Received 2 June 2017; Received in revised form 6 October 2017; Accepted 23 November 2017
Available online 23 November 2017
0939-6411/

surface charges and instability) and mainly by the harsh barriers of the gastrointestinal tract (GIT). Thus, INS undergoes conformational change/denaturation when in contact with the extremely acidic stomach fluid, followed by enzymatic digestion in the small intestine by the action of proteolytic enzymes, mainly trypsin and alpha-chymotrypsin, so that less than 0.1% of the INS dosage reaches the bloodstream in intact form [12]. Furthermore, the intestinal epithelium itself acts as a physical barrier against the permeation of the INS molecules, which in turn have high hydrophilicity and molecular weight, contributing to its reduced intestinal permeability [13].

In this work, we present a multi-strategy technological platform to enhance the oral bioavailability of INS, a BSC class III drug. The microencapsulation of INS seems to be a rational strategy for its protection against acid denaturation and enzymatic digestion, since its effective entrapment within the polymeric matrix should restrict the contact with H^+ ions from the gastric juice as well as with the proteolytic enzymes [14,15]. The gellan gum (GG) – a linear anionic polysaccharide and soluble in water – can be successfully used as encapsulating polymer because of its ability to form microparticles (MP) in the presence of multivalent cations [16,17]. The mucoadhesive properties of GG should also contribute to immobilization of MP in a target organ by a more intimate contact with intestinal epithelium (main absorption site) for extended periods of time, which favors the local concentration gradient, bypassing the drawbacks of intestinal permeability [18,19].

Several papers have shown that the colon is a favorable site for absorption of proteins/peptides [20–22], owing to its peculiar characteristics, such as pH near to neutrality, longer transit time and reduced activity of the proteolytic enzymes [23]. In this case, the colon-specific release of INS can be achieved by coating the INS-loaded MP with resistant starch/pectin (RS/P) films, which were previously developed and characterized in an earlier study published [24]. This is because the three-dimensional structure of such RS undergoes conformational alteration after being hydrothermally modified (retrogradation process) to a more ordered state in which the peptide bonds are protected from enzymatic attacks, conferring to this material high protective ability against digestion in the upper portions of the GIT. Upon reaching the colon, RS is specifically digested by the enzymes produced by the colonic microbiota, allowing the colon-specific release of INS [25]. It is important to highlight that the RS/P film coating can also exert an important role in the control of drug release kinetics.

Regarding the natural anionic polymers mentioned herein, there are important reports in the literature of their use for enhancing the absorption [26,27] as well as to inhibit the enzymatic digestion [28], which should represent an important alternative to conventional absorption enhancers and protease inhibitors, since many of them are toxic and act in a non-specific way. The aforementioned activities may be related to the calcium chelating activity, which plays an important role in the maintenance of intercellular contact, as well as being fundamental in the thermodynamic stability of the proteases [29,30].

On the basis of such premises, the aim of the present work was to encapsulate INS within mucoadhesive GG MP coated with RS/P films, as a promising strategy to overcome the problems of enzyme degradation and intestinal permeability, besides successfully releasing the drug in a specific gastrointestinal area (colonic delivery). In order to prove the interest of such formulation, it was necessary to evaluate (i) the protective effect of coated and uncoated MP against enzymatic degradation, (ii) the impact on permeability of INS both in Caco-2 cells and excised rat intestine, (iii) the release profiles of INS in dissolution media simulating the gastrointestinal tract conditions using flow-through cell apparatus (USP Apparatus 4) and (iv) the hypoglycemic effects in diabetic rats after oral administration.

2. Materials and methods

2.1. Materials

Pectin (type LM-5206CS – DE < 50%) and gellan gum (type Kelcogel® CGLA) were kindly provided by CP Kelco (Limeira, SP, Brazil). High amylose starch (HAS; type Hylon VII – 68% amylose) was a gift of the National Starch & Chemical (New Jersey, USA). Glycerin (99.5%), aluminum chloride ($AlCl_3$) and sodium chloride was purchased from Vetec (Duque de Caxias, Brazil). Human insulin solution (Novolin R 100 IU/mL) was obtained from Novo Nordisk A/S. Acetonitrile, trifluoroacetic acid (TFA), dimethylformamide (DMF), hydrochloric acid 37% v/v (HCl), phosphoric acid extra pure (H_3PO_4), sulfate sodium anhydre (Na_2SO_4), trypsin-EDTA, phosphate buffered saline (PBS), sodium hydroxide (NaOH), Dulbecco's modified Eagle's medium (DMEM), fetal bovine serum, vitamins, nonessential amino acids, L-glutamine, antibiotic solution (penicillin 100 IU/mL, streptomycin 10 mg/mL, and amphotericin B 25 μg/mL) and Hank's balanced salt solution (HBSS) were purchased from Fisher Scientific (Illkirch, France). Trypsin (11,800 U/mg) and α-chymotrypsin (59.3 U/mg) from bovine pancreas, N-benzoyl DL-arginine p-nitroanilide (BAPNA), N-benzoyl-L-tyrosine p-nitroanilide (BTPNA), Krebs Henseleit modified buffer and alloxan were purchased by Sigma Aldrich (Saint Quentin Fallavier, France). Transwell® Permeable Supports (Insert diameter 12 mm, 12 well, pore size 0.45 μm, insert membrane growth area 1.12 cm^2) and T-75 cm^2 flasks were purchased from Corning (Lowell, USA). Ketamine (Imalgene 1000®) was obtained from Merial laboratory, France.

2.2. Retrogradation of HAS mixed with pectin

The process of HAS retrogradation was carried out in two steps using alternating thermal cycles according to Meneguin et al. [24]. Briefly, aqueous dispersion of HAS at 5% (w/v) was gelatinized by autoclaving at 121 °C (120 min) and then mixed with pectin (5% w/v) at 1:1 ratio. After that, the dispersions were submitted to the retrogradation process by storage at 4 °C and 30 °C for 16 days (two days at each temperature) and after labeled as RS/P5.0 (patent no. BR 10 2016 028675 1).

2.3. Preparation of tested polymer dispersions

GG dispersions at 1.5 and 2.0% (w/v) (GG1.5 and GG2.0, respectively) were prepared by dispersing the polymer in heated water (60 °C) under constant magnetic stirring until complete homogenization.

For the further tests "Protective effect of MP against INS degradation" (Section 2.8.3) and "Transport experiments on Caco-2 cells" (Section 2.10.4), INS was added to all dispersions after the temperature cooled down until 37 °C, under mild magnetic stirring for 1 h, to a final concentration of 200 ug/mL. These INS-loaded dispersions were identified by adding the INS suffixes, as GG1.5-INS, GG2.0-INS, RS/P5.0-INS.

2.4. Microparticles preparation

MP were prepared by the ionotropic gelation technique. Briefly, GG aqueous dispersions (pH 4.5) at 1.5 or 2.0 (w/v) prepared according to Section 2.3 were dropped through 23G-gauze flat-tipped needle (25 × 0.6 mm) into a cooled solution of aluminum chloride (3 or 5%; *w/v*), containing INS solution (6.5% (*v/v*)) and respecting 1:1.3 GG dispersion:crosslinker ratio. MP were kept under magnetic stirring for 24 h to achieve maximum crosslinking and INS loading, followed by filtration and several rinsing with distilled water. After that, MP were dried at 25 °C for 24 h in an oven with forced air circulation and stored in a desiccator. Samples without INS were prepared as control (patent no. BR 10 2016 028675 1).

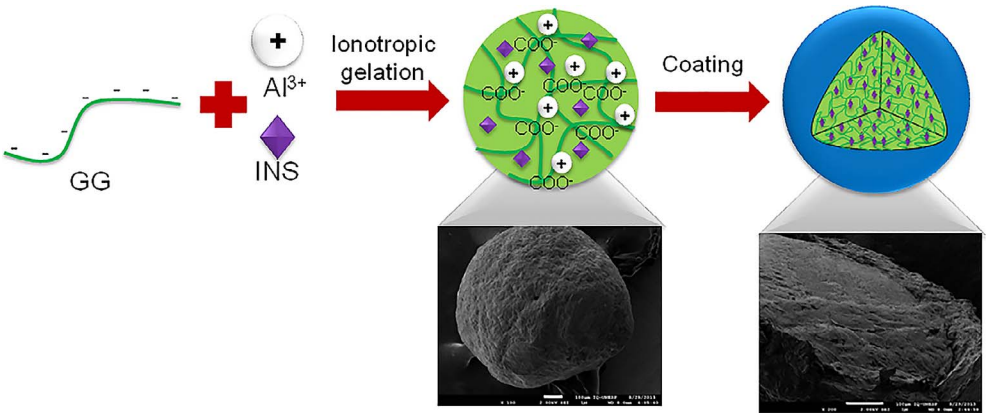

Scheme 1. Schematic representation of the coated INS MP preparation by ionotropic gelation technique using trivalent aluminum ion, which occurs through ionic bond with the carboxylate groups of glucuronic acid of gellan. Each ion of the crosslinker can bind with more than one carboxylic group, allowing more effective crosslinking.

2.5. Coating of MP using RS/P filmogenic dispersion

Filmogenic dispersion was prepared by adding 5% (w/v) of glycerin in relation to dry mass of polymers as plasticizer to the retrograded dispersion prepared in Section 2.2. MP were immersed in the RS/P dispersion for 1 min under gentle magnetic stirring, filtered and dried using cold air jet for 1 h (procedure repeated 2 times) (patent no. BR 10 2016 028675 1). MP without coating were obtained as control. A schematic representation of the coated MP preparation is shown in Scheme 1.

MP were labeled according to the concentration of GG (1.5 or 2.0%) and crosslinking solution (3 or 5% of $AlCl_3$) as 153 and 205. INS-loaded MP were added of INS prefix (INS153 and INS205) and those coated INS-loaded MP were added of C prefix (CINS153 and CINS205).

2.6. MP shape and size

The analysis of the shape and size of the MP were evaluated in stereoscope Leica MZ APO®, using the Motic Images Advances 3.2 software. The Feret diameter at 0° and the circularity were determined from the digitization of 100 MP images.

2.7. Encapsulation efficiency (EE%)

A known mass of MP was degraded into phosphate buffer solution (pH 7.4) under mild magnetic stirring for 24 h, followed by centrifugation at 5000 rpm for 10 min. INS concentration in the supernatant was measured by a reverse phase high performance liquid chromatography (RP-HPLC) and the EE% was defined as the total entrapped INS to total volume of INS solution absorbed, determined by swelling behavior according to Déat-Lainé et al. [27] for MP loaded by the diffusion method. Briefly, the volume of the absorbed solution was determined by swelling behavior, using dried and accurately weighed microparticles ($mass_0$ = 50 mg; n = 3) which were incubated in insulin solution (v = 2 mL) for 24 h and then, separated by filtration. The excess of liquid was carefully removed with absorbent paper, followed by weighing the wet masses. For the better appreciation of the results, the amount of encapsulated INS was also expressed as INS loading (Eq. (1)) and INS concentration (IU per 200 mg of MP).

$$INS\ loading = \frac{mass\ of\ INS(\text{mg})\ in\ 100\ \text{mg}\ of\ MP}{100\ \text{mg}\ of\ MP} \times 100 \quad (1)$$

The HPLC protocol consisted of a reverse-phase RP-HPLC (Merck-Hitachi) equipped with an intelligent pump (L-62000 A), a diode array detector (L-45000) and an interface (D-6000). The LiChrospher RP-18 column (5 µm, 4 mm × 250 mm, Merck, Darmstadt, Germany) equilibrated at 40 °C with a flow rate of 1.0 mL/min was used. The mobile phase consisted of 0.2 M sodium sulfate buffer (pH adjusted to 2.3 with phosphoric acid) and acetonitrile (72:28). The injection volume was 20 µL via an autosampler (AS-2000 A) and the run time was 12 min. The absorbance of the INS was recorded at 214 nm and the area under the curve was used for calculation of INS concentration based on the calibration curves.

2.8. Inhibitory activity of MP against proteolytic enzymes

2.8.1. Inhibition of the trypsin

Effects of polymeric dispersions (GG1.5, GG2.0 and RS/P5.0), coated (C153 and C205) and uncoated control MP (153 and 205) on enzymatic activity was studied with trypsin and alpha-chymotrypsin according to Ameye et al. [31]. Briefly, BAPNA was dissolved in DMF (20 mM) as a substrate solution. The samples were dispersed in phosphate buffer (0.2 M, pH 7.4) at 1% (w/w) and 1 mL of dispersions was immediately mixed with substrate solution (1:1 ratio). Trypsin (30 IU/mL) previously prepared in 10 mM HCl was added and the samples were incubated at 37 °C for 30 min. Enzymatic action was stopped by the addition of 1% trichloroacetic acid solution and the metabolite p-nitroaniline was quantified by measuring the absorbance at 405 nm. Control experiments were performed in a similar way without MP addition and the enzyme activity found ($EA_{control}$) was assumed as 100%. The enzymatic inhibition of trypsin was calculated according to Eq. (2):

$$\%\ Enzymatic\ inhibition = (EA_{control}/EA_{samples}) \times 100 \quad (2)$$

The experiments were made in triplicate.

2.8.2. Inhibition of the alpha-chymotrypsin

Briefly, BTPNA was dissolved in DMF (1.18 mM) as a substrate solution. The samples (GG1.5, GG2.0 and RS/P5.0 polymeric dispersions, C153 and C205 coated MP and 153 and 205 uncoated MP) were dispersed at 1% (w/w) in Tris-HCl buffer (10 mM, pH 7.8) containing alpha-chymotrypsin (40 IU/mL). 1 mL of these dispersions was immediately mixed with substrate solution (1:1 ratio) and the set was incubated at 37 °C for 30 min. After this, the enzyme reaction was stopped with 1% (v/v) trichloroacetic acid and the enzymatic inhibition of alpha-chymotrypsin was calculated according to Eq. (2). The experiments were made in triplicate.

2.8.3. Protective effect of MP against INS degradation

The ability of MP to protect the encapsulated INS against enzymatic degradation was evaluated by dispersing INS-loaded MP (INS153, CINS153, INS205 and CINS205) in phosphate buffer (0.1 M; pH 7.4) at a concentration of 100 µg/mL and containing trypsin (10 IU/mL) and alpha-chymotrypsin (10 IU/mL). The set was incubated at 37 °C during 120 min and aliquots were withdrawn at predetermined times (0, 30, 60, 90 and 120 min) followed by the addition of aqueous solution of TFA (0.1% v/v) in order to stop the enzymatic reaction. The INS concentration in the buffer was quantified by RP-HPLC at 214 nm. A similar test with INS solution (Free-INS) was performed for comparison. All

experiments was performed in triplicate.

2.9. In vitro release studies using flow-through cell system (USP apparatus 4)

INS dissolution tests from coated (CINS153 and CINS205) and uncoated (INS153 and INS205) MP were performed with an automated flow-through cell dissolution apparatus (USP apparatus 4, Sotax CE7 smart, Switzerland) using 100 mL of hydrochloric acid for 1 h (0.1 N; pH 1.2), acetate buffer for 1 h (0.1 M; pH 4.5) and phosphate buffer for 5 h (0.1 M; pH 6.8), mimicking the pH values along the gastric, duodenal and colonic portions. Experiments were performed at 37 ± 0.5 °C and flow rate of 24 mL/min in a closed loop configuration. Flow through cells (12 mm inner diameter) were filled with glass beads (1 mm) and one ruby bead (about 5 mm diameter) was located at the apex. The dissolution media was pumped through the cells and returned to the reservoir vessels with a piston pump (CY 7–50, Sotax, Switzerland). Aliquots (1 mL) were withdrawn at pre-determined times and the same volume was replaced with fresh medium. INS release was quantified in HPLC at 214 nm. All experiments were performed in triplicate.

2.9.1. Release kinetic models

The release data recorded in Section 2.9 were fitted to different mathematical models (Baker-Londsdale, First Order, Higuchi, Hixson-Crowell, Korsmeyer-Peppas and Weibull) according to the Eqs. (3)–(8), respectively. All equations were fitted to the 100% dissolution curves, except for Peppas (60%) and Weibull (62.3%) equations.

$$f = 3/2[1-1-(f/100)^{2/3}]-(f/100) = K_{BL}t \quad (3)$$

$$f = 100(1-e^{k_1 t}) \quad (4)$$

$$f = k_H\sqrt{t} \quad (5)$$

$$f = [1-(1-k_{HC}t)]^3 \quad (6)$$

$$f = k_p t^n \quad (7)$$

$$f = 1-\exp(-at^b) \quad (8)$$

where f corresponds to the amount of drug release at time t; k_{BL}, k_1, k_H, k_{HC} and k_P are constants of release rates, and n and b are exponents of release.

2.10. Cell-based studies

2.10.1. Caco-2 cell culture

The Caco-2 human colon cancer cells from American Type Culture Collection (ATCC, Rockville, MD) were cultured in T-75 cm^2 flasks containing DMEM supplemented with glucose (4.5 g/L), FBS (20%; v/v), vitamins (2%; v/v), nonessential amino acid solution (2%; v/v), L-glutamine (2%; v/v) and antibiotic solution (2%; v/v), at 37 °C in a humidified atmosphere of 5% CO_2/95% air. The medium was changed every 3 days until cells reach 80–90% confluency when they were split using trypsin-EDTA. Caco-2 cells from passage number 25–30 were seeded at a density of 1×10^5 cells/well on the T12 filter inserts Transwell® (pore size of 0.4 μm and growth area of 1.13 cm^2) and cultured for 21 days when Caco-2 cells exhibited differentiation. The medium was changed every day. Before initiating the tests, the medium was removed, and the cell monolayer was washed three times with 37 °C PBS (1 mL).

2.10.2. Transepithelial electrical resistance (TEER) measurement

Before initiating the transport tests, the medium was removed, followed by washing off with PBS (3×) the Caco-2 cell monolayers, which were incubated with HBSS for 1 h (37 °C; 95% air/5% CO_2) allowing their stabilization. The integrity of the monolayers was evaluated by TEER measurement on polycarbonate filter membranes with electrode STX2, EVOMX World Precision Instruments (Sarasota, FL, USA). The cell monolayers with TEER > 800 Ω cm^2 were selected for the permeation studies across cells monolayer and TEER was monitored during all test for 120 min [27].

In order to check the recoverability of cells to original impermeable state, after the permeation assay the samples were removed from monolayers, which were washed with PBS (2×), followed by the culture medium addition. After 30 min of stabilization, new measures of TEER were made during 24 h.

2.10.3. Cytotoxicity of polymers and MP

Caco-2 cells were seeded on 24-well plates containing supplemented DMEM at density of 2.5×10^4 cells/well and grown for 5–6 days. After the monolayer formation, cells were incubated with Free-INS, INS-polymer dispersions (GG1.5-INS, GG.2.0-INS, RS/P5.0-INS) or MP (CINS153, CINS205, INS153 and INS205) (concentration of INS = 100 μg/mL) for 120 min, at 37 °C in an atmosphere of 95% air/5% CO_2 at 90% relative humidity. Samples were carefully removed and the cells monolayers rinsed with PBS (2×) for incubation with trypan blue (0.1%; v/v, in PBS at 37 °C). Monolayers were examined by inverted microscope for dye exclusion. Data were expressed as the percentage of viable cells [32,33].

2.10.4. INS permeability on Caco-2 cells

INS permeability tests across the Caco-2 cells monolayer was carried out from the apical to basolateral direction in HBSS pre-equilibrated at 37 °C for 1 h according to Déat-Lainé et al. [27]. For the experiments, Free-INS (100 μg/mL), polymeric dispersions (GG1.5-INS, GG2.0-INS, RS/P5.0-INS) (100 μg/mL), coated and uncoated MP (CINS153, CINS205, INS153 and INS205) suspended in HBSS (100 μg/mL) were added to the insert apical chamber and the plates were incubated at 37 °C during 120 min. 50 μL was withdrawn from the basolateral compartment at different times (0, 15, 30, 60, 90 and 120 min) and the media was immediately replaced with fresh HBSS. The INS permeated across Caco-2 cells monolayer was quantified by RP-HPLC at 214 nm. All experiments were performed in triplicate. The apparent permeability coefficient (P_{app}) was calculated according to Eq. (9):

$$P_{app}(\text{cm}\cdot\text{s}) = (dQ/dt) \times (1/A \times C_0) \quad (9)$$

where dQ/dt is the flux of the sample across the monolayer (μg/s), C_0 is the initial concentration in the apical compartment (μg/mL), and A is the surface area of the monolayer (1.12 cm^2).

Absorption enhancement ratios (R) were obtained from Eq. (10), as follow:

$$R = (P_{app(sample)}/P_{app(control)}) \quad (10)$$

2.11. Animals studies

All animal procedures were performed in compliance with the 'Principles of Laboratory Animal Care' of the US National Institute of Health (NIH). Animal studies were carried out at Université Clermont Auvergne (Clermont Ferrand, France) and approved by the CEMEA Auvergne Research Ethics Committee (Clermont-Ferrand, France). Additional studies were performed at São Paulo State University (UNESP) (Araraquara, Brazil) approved by the Ethics Committee on the Use of Animals of the São Paulo State University (protocol CEUA/FCF/CAr n° 47/2012).

Adult male Wistar rats (200–250 ± 20 g) were housed under controlled environmental conditions regarding humidity and temperature (22 ± 3 °C) with a 12:12 h light/dark cycle. Animals were fasted 24 h prior to experiments, but they had free access to water (*ad libitum*).

2.11.1. Ex vivo INS permeability on intestinal rat tissues

Rats were anesthetized with an intraperitoneal injection of

ketamine at a dose of 0.15 g/kg of body weight. The colon of each rat was quickly removed and serosal side was rinsed with 10 mL of 0.9% NaCl at 37 °C. One end was closed using suture wire. Each of samples Free-INS and MP (CINS153, CINS205, INS153 and INS205) containing the same amount of INS was incubated into the intestinal sac. The other end of the intestinal segment was closed and sacs were incubated into a tissue chamber containing 12 mL of Krebs Henseleit modified buffer (composition in mmol/L: 118.1 NaCl, 4.7 KCl, 2.2 $CaCl_2{\cdot}2H_2O$, 1.2 $MgSO_4$, 1.2 KH_2PO_4, 25.0 $NaHCO_3$, and 11.1 glucose, pH 7.5) at 37 °C and oxygenated (95% O_2/5% CO_2) for 180 min (maximum viability for rat material). At predetermined times (30, 60, 90, 120, 150 and 180 min), aliquots (200 µL) were withdrawn and replaced by fresh medium maintained at same temperature. The amount of INS permeated was quantified by RP-HPLC at 214 nm.

The apparent permeability coefficient (P_{app}) was calculated according to Eq. (9), where dQ/dt is the INS flux from the mucosal to the serosal side of the mucosa (µg/s); C_0, the INS initial concentration in the lumen compartment (µg/mL) and A is the membrane area (cm^2), which corresponds to $A = length \times diameter$. The absorption enhancement ratio was calculated according to Eq. (10).

2.11.2. In vivo hypoglycemic effect on diabetic rats

Diabetes was experimentally induced in male Wistar rats by an intraperitoneal injection of aloxane (140 mg/kg) dissolved in 0.9% saline as previously described by Kumar et al. [12]. The blood glucose levels were checked after 48 h using a glucose meter (OneTouch® Select Simple™) by collection blood from the tail vein. Animals with blood glucose ≥300 mg/dL were selected for the study. Diabetic rats were divided into 8 groups of 6 rats. Animals were fasted overnight, prior to the start of experiments.

Negative control group received MP without INS, while the positive control group received subcutaneous injection of INS (Novolin R®) at the dose of 10 IU kg^{-1}. The other groups received INS-loaded MP (CINS153, CINS205, INS153 or INS205) immediately after their suspension in distilled water (100 IU kg^{-1}) through an adaptation of the oral gavage technique with the aid of a polyethylene tube. The blood glucose level (BGL) was checked at predetermined intervals (0, 30, 60, 120, 180, 240, 300, 360 and 420 min) during 7 h. The BGL reduction (% of initial) was calculated from the curve blood glucose concentration *versus* time using the Eq. (11):

$$BGL_{reduction} = [(G_0 - G_t)/G_0] \times 100 \quad (11)$$

where G_0 is the fasting glucose level (mg/dL) and G_t is the plasma glucose level at time (t) after oral administration of the samples.

2.12. Statistical analysis

Each value was expressed as the mean ± SD. When applied, the results were treated by one-way analysis of variance (ANOVA) to assess the significance of the differences between data. Tukey–Kramer post-test was used to compare the means of different treatment data (GraphPad Prism 5 software). Results with $p < .05$ were considered statistically significant.

3. Results and discussion

3.1. MP preparation

MP were obtained by the ionotropic gelation technique due to some favorable features of GG, such as hydrophilicity and presence of free anionic groups which bind ionically with cations promoting the gelatinization and aggregation [17]. Although the crosslinking of MP using Ca^{2+} is quite exploited [34–36], recent studies have shown that the higher valence of Al^{3+} allows a more extensive crosslinking of polymer, resulting in a more effective control of drug release rates [17].

Contrary to the claim made by Maiti et al. [17], it was possible to prepare GG MP in concentrations above 1.25% (1.5 and 2.0%) by applying temperature (60 °C) in order to reduce the GG dispersions viscosity. According Prezotti et al. [16], GG degradation occurs only at temperatures above 230 °C, which leads us to conclude that the temperature applied during the dripping phase does not interfere with the thermal properties of the final MP.

During the MP preparation, it was observed that some operational parameters strongly influence the final properties of the MP. Important examples of this were the polymeric dispersions dripping at low collection distance (about 1 cm of the crosslinking solution surface) and the high stirring speed (720 rpm) applied during MP crosslinking, which made possible to reach particles with more circular shape and homogeneous size. When a dispersion is dripped at lower heights, its drops assume slower speeds during falling, minimizing the impact of drops with liquid surface, which should preserve the shape of the original drop, besides avoiding shape irregularities such as MP with tail [37]. Furthermore, the round shape of MP is also result of the shearing that the crosslinking solution at high stirring speed causes on the particles surface, having a polishing effect on them.

3.2. Size/shape of MP

GG MP presented a good sphericity (0.69–0.76) with average particle sizes ranged from about 1000–1200 µm (Table 1). The larger diameter found for 205 MP (~1197 µm) in relation to 153 MP (~1033 µm) ($p < .05$) is a consequence of the highest gellan concentration employed (2.0%) that forms a more viscous dispersion with increased surface tension, building bigger droplets during the dripping phase, and thus bigger MP [38]. After INS incorporation, a significant decrease in size of INS205 MP (1065 µm) in relation to its counterparty 205 MP(~1198 µm) ($p < .05$) was verified, which can be related to the strong drug-polymer interaction responsible for the polymeric network shrinkage [39,40]. However, no significant difference ($p > .05$) was observed between the 153 (1033 µm) and INS153 MP (1054 µm) probably because of the higher amount of INS encapsulated (see Section 3.3) that fills the interstitial spaces of polymer network and keeps the structures expanded.

According to the values of circularity presented at Table 1, MP obtained in this work by ionotropic gelation can be considered approximately circular, since the values recorded for this parameter were close to 1. The incorporation of INS favored the circularity of MP perhaps because the drug molecules occupy the void interstitial spaces,

Table 1
Results of size (µm), circularity, EE (%), INS loading and INS concentration (UI/200 mg) of GG MP prepared by ionotropic gelation. The results are presented as mean ± standard deviation (n = 100 for size and circularity, and n = 3 for EE and drug loading).

MP	Size (µm)	Circularity	EE (%)	INS loading (%)	INS concentration (UI/200 mg)
153	1033 ± 102	0.69 ± 0.17	–	–	–
205	1197 ± 102	0.69 ± 0.17	–	–	–
INS153	1054 ± 78	0.76 ± 0.07	91 ± 2	0.99 ± 0.02	57.14
INS205	1065 ± 92	0.73 ± 0.06	57 ± 3	0.68 ± 0.01	38.85
CINS153	1066 ± 69	0.75 ± 0.09	89 ± 2	0.98 ± 0.03	56.43
CINS205	1079 ± 87	0.74 ± 0.08	55 ± 3	0.65 ± 0.02	37.11

avoiding that the shrinkage occurs in a heterogeneous way, as evidenced earlier [16].

3.3. INS encapsulation efficiency (EE%)

EE% and INS loading of the GG MP is shown in Table 1. INS loading ranged from 0.65% to 0.99%. For INS153 and INS205 MP, the INS loading efficiency was about 91 and 57.8%, respectively. Although the increase of the polymer concentration is often associated with the raise of the EE% because of the greater number of functional groups to interact with the drug molecules [41], MP prepared with lowest GG concentration (1.5%) showed an increment of about 33% of INS entrapped. This behavior can be attributed to the building of less packed and dense structures that facilitates the INS diffusion into the MP during the loading process as a consequence of the lowest GG and Al^{3+} concentrations used. Furthermore, the use of low crosslinking concentrations avoids the water expulsion followed by the convective loss of drug molecules during the crosslinking process [17,42].

On the other hand, the charge transformation of INS played an important role for the INS loading efficiency. The net charge of INS became positive on crosslinking solution, since its pH value (pH = 4.5) was always below the isoelectric point of INS (pI = 5.35–5.45), which must have favored the electrostatic interactions with the negative carboxylic groups (COO^-) of GG, thus increasing the INS entrapment [43].

For a relation EE% *versus* oral dosage, as previously purposed by Tahtat and coworkers [44], the amount of encapsulated INS was expressed in IU per 200 mg of MP (IU/200 mg) (Table. 1). Taking into account that 1 IU equals to 0.035 mg of INS, and its therapeutic dosage corresponds to 0.5–1 IU/kg per day administered in 2 or 3 doses, for a diabetic patient with body weight of 60 kg, the dosage required to achieve the glycemic effect should be 30–60 IU/day, *i.e.*, 10–20 IU/administration. Thus, the mass of MP proposed (200 mg) for the both INS153 or INS205 can provide from 1.9 to 2.8 times more INS than the dosage required.

The fastness of the MP coating process by immersion in RS/P filmogenic dispersion for only 1 min did not lead to a significant decrease of EE% ($p > .05$).

3.4. Inhibitory activity of control MP against proteolytic enzymes

As the enzymatic degradation of proteins/peptides in the gastrointestinal environment represents one of the greatest barriers to their oral administration, this study had as one of its main objectives to evaluate the enzyme inhibitory effect of the MP. Trypsin and α-chymotrypsin were used as enzyme models, since they are considered the major enzymes involved in protein digestion by the peptide bonds hydrolysis after their activation in the duodenum [45]. Although the use of traditional protease inhibitors is a promising strategy to support the oral administration of proteins/peptides, these substances may act unspecifically most often and even alter physiological secretion of proteases [20]. Unlike, the use of protease inhibitors polymers are more economical and present low systemic absorption, which contributes to decrease of the side effects and toxic, besides presenting mucoadhesive and penetrating properties [28,46].

The inhibition of trypsin and chymotrypsin exerted by the polymer dispersions and MP without INS is shown in Fig. 1A. For the dispersions (GG1.5, GG2.0 and RS/P5.0), the inhibition values were found between 5 and 13%. However, no statistically significant differences were observed between these samples ($p > .05$).

MP showed greater efficacy to inhibit the proteolytic activity than the polymer dispersions, reaching values of 64% for trypsin and 62% for α-chymotrypsin. The increasing of the GG concentrations from 1.5 to 2.0% favored the trypsin inhibition ($p < .05$), probably due to the formation of a more viscous gel, which constitutes a physical barrier against the diffusion of the enzyme to the BAPNA substrate, besides blocking the enzymatic active site [47]. Furthermore, MP present a

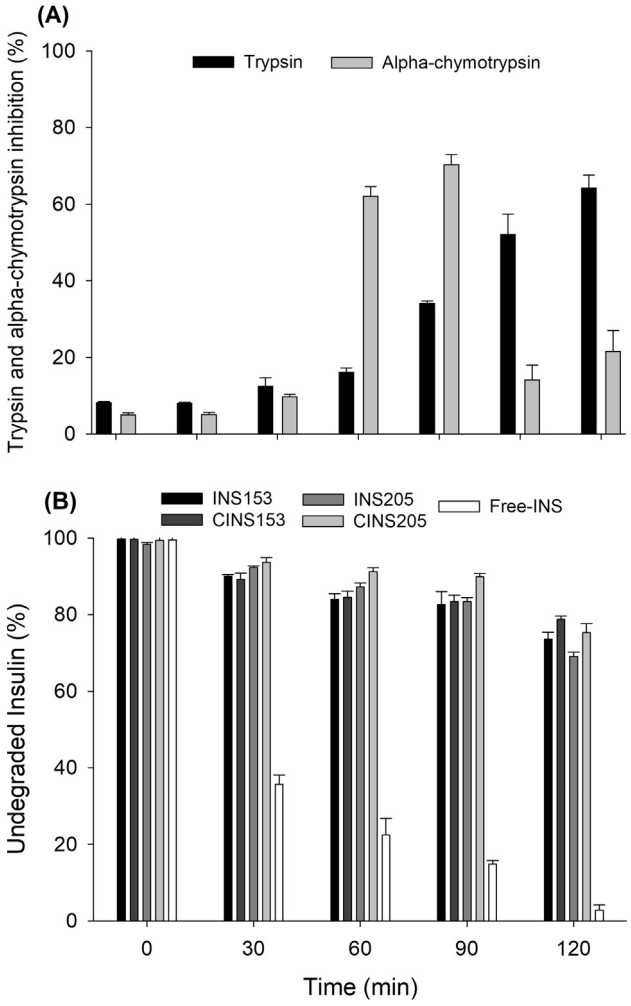

Fig. 1. (A) *In vitro* trypsin and alpha-chymotrypsin inhibitory effect of polymer dispersions (GG1.5, GG2.0 and RS/P5.0) and control MP (153, C153, 205 and C205) and (B) Amount of intact INS (%) during the degradation studies from INS solution (Free-INS) and INS encapsulated into MP (coated and uncoated) (mean ± SD; n = 3).

crosslinked matrix by presence of both RS/P (physic crosslinking) and Al^{3+} (ionic crosslinking) in which the substrates remain embedded and thus protected from degradation. According to LV and co-workers [28], the higher concentration of polymer is also responsible for a greater electrostatic interaction polymer-enzyme, decreasing the amount of free enzyme as well as the optimal pH for the enzymatic activity.

On the other hand, Ca^{2+} plays a key role in the thermodynamic stability of proteases, which have binding sites for this ion [28]. In this sense, the ability of some polymers, such as those used in this study, to bind to calcium is another mechanism of proteases inhibition that occurs by enzyme denaturation and is dependent on the distance between the carboxyl groups constituent of the polymer [48], as well as its crosslinking degree [30].

In contrast to the above behavior, 153 and C153 MP (lowest GG and Al^{3+} concentrations) were more efficient to inhibit chymotrypsin, suggesting the existence of different mechanisms of inhibition. In fact, the enzymatic activity depends on its original structure and polarity, so that the addition of other compounds as polymers and crosslinkers can lead to several types of interaction, as well as conformational changes, contributing to the reduction of the catalytic activity.

Interestingly, we hypothesize that the more organized and coiled tridimensional structure of RS in the form of double helices stabilized by hydrogen bonds [25] has played an important role in enzymatic inhibition, so that C153 and C205 MP offered an additional inhibition ranging from 18.7 to 52.9% for trypsin and11.4 to 33.3% for

chymotrypsin, respectively.

3.5. Evaluation of protective effect of MP against INS degradation

As can be observed in Fig. 1B, Free-INS was extensively degraded by trypsin and chymotrypsin so that only 36% remained intact after 30 min of test and this value decayed to about 3% in the next 120 min. On the contrary, the microencapsulation of INS allowed its effective protection against degradation, resulting in up 70–80% of INS protected until the end of the test. Such behavior is not only the result of the physical barrier that protects the entrapped INS into MP [13], but may also be related to the building of a gel layer around the MP that hinders the diffusion of enzymes towards the substrate (INS).

After 120 min of test, INS153 and CINS153 MP had a slightly higher protective effect than those samples prepared with higher concentrations of polymer and crosslinker (INS205 and CINS205) ($p < .05$). It was suggested that the more flexible polymer chains, as a result of the more gentle physical and ionic crosslinking, made the functional groups more available to interact with the enzymes, leading to conformational changes and hence decreasing of activity. Furthermore, the looser polymer network favors the liquid entrance, so that the swollen layer on the surface of MP is formed quickly, protecting the INS against degradation since the start of the test, reducing the total percentage of INS degraded.

In order to keep constant the INS concentration during the tests, making possible the evaluation of the influence of carrier system concentration on the protection against the enzymatic degradation, different MP masses were used based on their EE%. As shown in Fig. 1, the samples containing a lower mass of polymer (INS153 and CINS153, higher EE%) presented a slight increasing of protective activity against trypsin and chymotrypsin, corroborating the finding that a looser polymer network may favor both the interaction with the proteolytic enzymes and the formation of a gelled layer that restricts the enzymatic diffusion.

3.6. In vitro INS release studies using flow-through cell system (USP apparatus 4)

INS release profiles from coated and uncoated MP in media that simulate the gastric (pH 1.2), duodenal (pH 4.5) and colonic (pH 6.8) pH are shown in Fig. 2. The CINS153, INS205 and CINS205 samples released lower amounts of INS at pH 1.2 (32, 37 and 18%, respectively) and pH 4.5 (14, 22 and 14%, respectively) than in phosphate buffer pH 6.8 (53, 40 and 67% respectively), demonstrating a pH-dependent behavior that can be successfully exploited for the targeted release. Such behavior is related to the influence of pH on the ionization of the anionic polymers, so that in acid media their carboxyl groups are protonated, promoting the electrostatic interaction of the polymer chains, which become tighter and thus hinder the penetration of liquids and the subsequent dissolution/diffusion of drug molecules [49,50].

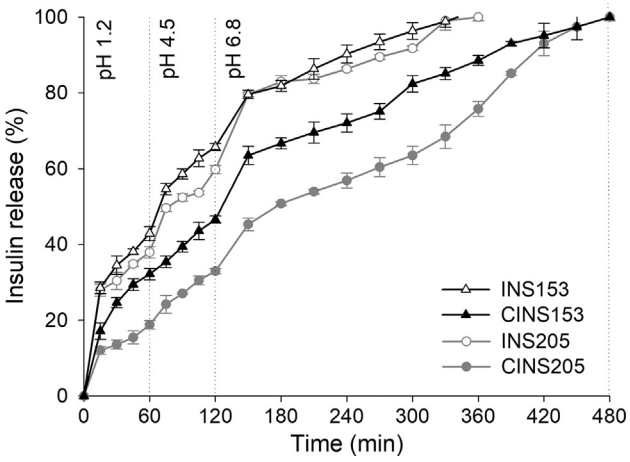

Fig. 2. *In vitro* INS release profiles from coated and uncoated MP in media with different pH values, mimicking gastric (0–60 min; pH 1.2), duodenal (60–120 min; pH 4.5) and colonic (120–480 min; pH 6.8) phases. Each value represents mean ± standard deviation, n = 3.

At acid media, INS was released faster from INS153 (~42%) than other samples, demonstrating again that less crosslinked polymer networks experience greatest chains flexibility, which contributes to the diffusion of drug molecules. Maiti and co-workers [17] in their studies with GG MP also related a faster glipizide release when lowest amounts of crosslinking were used.

The burst release in the first 15 min of the test (about 12–28%) was attributed to the INS adsorbed on the surface of MP [51] and its high solubility at low pH values. Besides, at pH lower than its isoelectric point, the INS is negatively charged [43], leading to electrostatic repulsion between the polymers and the INS [47]. However, taking into account that INS remains almost completely undegraded within the first 15 min of incubation with trypsin and chymotrypsin, the burst effect of release may be important to control the postprandial blood glucose, in which an immediate effect is expected.

The effectiveness of the coating was evidenced by the lowest INS release rates from CINS153 and CINS205, with a significant reduction in acid (24.9–50.5%) and acetate buffer (34.9–37.1%). Regarding the time required to release 100% of the drug, coated MP were able to sustain the drug release up to 480 min ($p > .05$), while 100% of released INS from INS153 and INS205 was reached in 330 min and 360 min, respectively ($p < .05$). These results are in accordance with those found in our previous work about the development of the RS/P free films [24], in which the dissolution data were also lower in acid media (~24%) than in phosphate buffer (pH 7.4) (~ about 45%). Herein, the data shown reflect the more packed and crystalline three-dimensional structure of the RS and its low water solubility [52], in addition to the ability of pectin to form a thick viscous layer which hinders the drug molecules diffusion [53].

3.6.1. In vitro INS release kinetics

Different mathematical models were applied to drug release profiles (Fig. 2) and the correlation coefficients (r^2) were determined, which are shown in Table 2. The INS release data from INS153 and CINS205 correlated better with the Korsmeyer-Peppas (r^2 = 0.9786 and 0.9823, respectively). This model is based on the Power Law and relates exponentially the drug release with time (Eq. (6)) [54]. As the release exponents (n) ranged between 0.43 and 0.85, the release mechanism followed non-Fickian diffusion (or anomalous transport), in which the diffusion and polymeric chains relaxation processes driven the drug

Table 2
Release coefficients of mathematical models (Baker-Lonsdale, Higuchi, Korsmeyer-Peppas, First order, Hixson-Crowell and Weibull) from coated and uncoated MP.

Mathematical models		Samples			
		INS153	CINS153	INS205	CINS205
Baker-Lonsdale	k	0.0010	0.0006	0.0009	0.0004
	r^2	0.9756	0.9496	0.9520	0.8563
Higuchi	k	5.7889	4.6327	5.5517	3.9410
	r^2	0.9766	0.9900	0.9742	0.9234
Korsmeyer-Peppas	k	7.0203	2.9845	7.0913	0.8846
	r^2	0.9786	0.9627	0.9716	0.9823
	n	0.4666	0.5881	0.4386	0.7217
First order	k	0.0102	0.0060	0.0089	0.0040
	r^2	0.9740	0.9802	0.9652	0.9558
Hixson-Crowell	k	0.0027	0.0016	0.0024	0.0011
	r^2	0.9543	0.9691	0.9516	0.9730
Weibull	k	98.59	99.39	98.58	124.90
	r^2	0.9714	0.9799	0.9678	0.9788
	b	1531	1342	939	678.30

release.

Unlike, CINS153 and INS205 had the best correlation with Higuchi model (r^2 = 0.9900 and 0.9742, respectively), indicating that the drug release from matrix system was diffusion controlled according to the Fick Law, in which the diffusion is driven by a concentration gradient.

3.7. Permeability studies using Caco-2 cell monolayers

In this work, INS – a drug class III according to BCS (Biopharmaceutical Classification System) – was carried in coated mucoadhesive MP prepared with natural polysaccharides from renewable sources aiming the improvement of its intestinal permeation and possibly of its bioavailability. In this sense, the determination of the INS permeation properties from MP (coated and uncoated) is fundamental to predict the *in vivo* performance.

3.7.1. Transepithelial electrical resistance (TEER)

TEER measurement has been considered a valuable bioelectrical tool to check the cell monolayer integrity and consequently to predict the paracellular transport of some drugs, since it express the tightness of tight junctions (TJ), which are located between adjacent epithelial cells [55,56].

Fig. 3 shows the TEER profile of the cell monolayers incubated with polymer dispersions and MP during the permeation assay. Among the dispersions, RS/P5.0-INS reduced TEER values (approximately 27%) after 120 min of test, whereas no decrease was observed for GG1.5-INS and GG2.0-INS ($p > .05$). In fact, the RS/P blend forms a more packed and dense network resulting in a configuration that may favor the interaction with the TJ proteins and/or receptors, favoring their opening as previous demonstrated for chitosan [57].

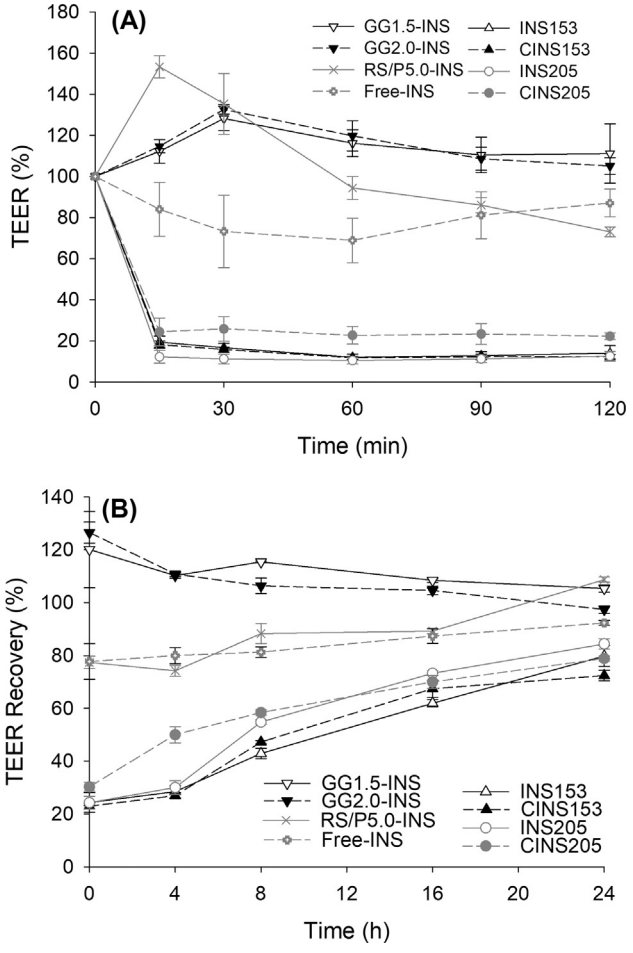

Fig. 3. TEER-time profiles of Caco-2 cells for polymer dispersions (GG1.5-INS, GG2.0-INS and RS/P5.0-INS), MP (INS153, CINS153, INS205 and CINS205), Free-INS and control (mean values ± SD; n = 3) evaluated (A) during permeability tests (120 min) and (B) after samples removal (mean values ± SD; n = 3).

All MP promoted an immediate and significant reduction of the TEER values of Caco-2 cell monolayers in relation to the control ($p < .05$). About 88% of reduction of TEER values was reached until 15 min of the test, when these values reached the equilibrium until the end of the test (120 min). This finding suggests that the MP developed promoted the opening of TJ, making them a promising strategy for increasing the permeability of hydrophilic drugs through the paracellular route [58] like as proteins.

As the MP had different EE% (see Section 3.3), it was expected that those samples evaluated in greater amount (INS205 and CINS205) in order to guarantee the same INS concentration would favor the reduction of TEER, and consequently, the opening of the TJ. However, CINS205 was the less effective in reducing TEER (~77%) ($p > .05$), while for the other samples no statistically significant differences were observed ($p < .05$).

Concerning to TJ opening, some natural polymers interact with proteins of TJ or surface receptor, causing its detachment [59]. Besides, anionic polymers acts as calcium chelating, leading to rupture of adherens junctions (another kind of cell-cell adhesion) and TJ, since Ca^{2+} is essential for maintaining the cells functionality [29].

Regarding particle size and its influence on permeation optimization, it is known that nanosized particles favor the interaction with the TJ mainly due to their greater surface area. However, the micrometric size of the particles developed in this work should not be taken as a disadvantage, since these samples were prepared from gellan gum, a polymer with remarked mucoadhesive properties, which attach to the mucosal surface leading to the rapidly TJ opening [60].

Importantly, after removal of samples from Caco-2 cells monolayers, it was verified a gradual recovery of TEER values in relation to the baseline levels, which ranged from 72 to 108 after 24 h, indicating that the impressive effect of samples on TJ opening is reversible.

3.7.2. MP cytotoxicity on Caco-2 cells

Cell viability test by the technique of trypan blue exclusion was used to analyze the cytotoxicity of the polymers as well as their MP. According to presented in Fig. 4B, the Caco-2 cells viability was higher than 95% after 2 h of contact with the all samples, indicating that the developed systems are biocompatible [27]. A lowest cell viability was found for Free-INS (about 93%), suggesting that the microencapsulation has played an important role in reducing INS cytotoxicity.

3.7.3. INS permeability on Caco-2 cells

The apical-basolateral passage was significantly increased when the INS was transported from the MP, so that the permeation rates ranged from 42 to 67% (Fig. 4A) against only 25% of the Free-INS. The values of P_{app} (Table 3) reached 48×10^{-6} cm s^{-1} which is considered a sufficiently high value to the mannitol (P_{app} values of 0.12×10^{-6} cm s^{-1}), a substance widely used as a marker of paracellular transport in Caco-2 cells [54]. These data are consistent with the significant reduction of TEER values previously observed.

By comparing the values of INS permeation from samples CINS153 (~67%) and INS153 (~42%), both prepared with 1.5% GG, it is possible to note that the RS/P coating favored the permeation across the cells ($p < .05$). However, for MP prepared with the highest concentration of polymer (2.0%), a distinct behavior was detected in which INS205 (~57%) presented high permeation than sample CINS205 (~45%). It can be thinking that both the coating and the high concentrations of GG and crosslinker in the sample CINS205 made the INS release low in 120 min of the test, so that a reduced amount of INS was available in the apical compartment to permeate the Caco-2 monolayer. This finding is in agreement with the INS release results (Section 3.6), in which CINS205 promoted the greater control of the INS release rates.

Polymer dispersions also promoted the increase of INS permeability

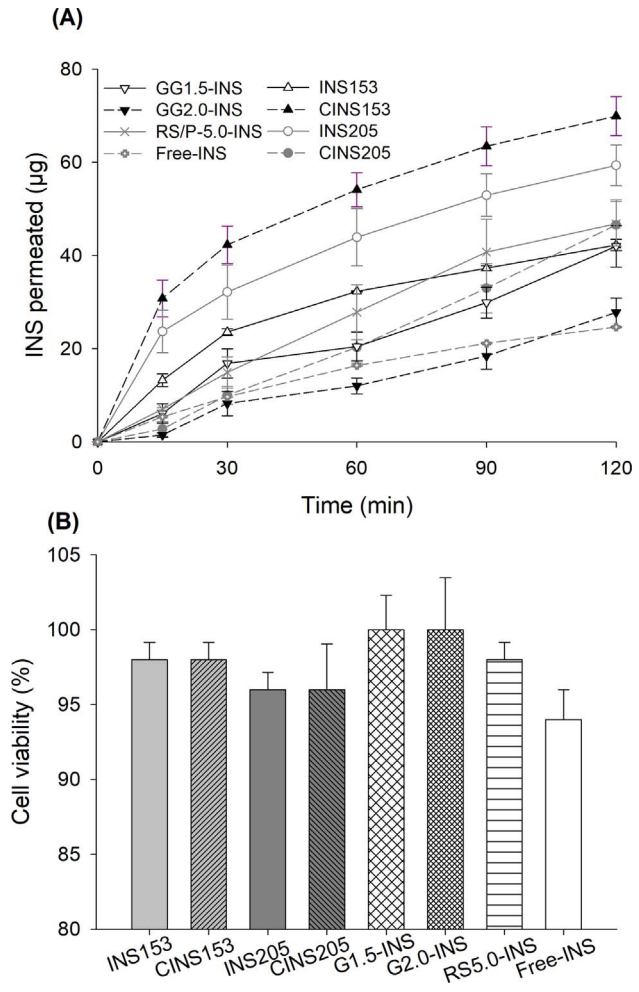

Fig. 4. (A) INS permeability on Caco-2 cells monolayers (*ug*) from polymer dispersions and MP and (B) Caco-2 viability (%) after incubation with control (no treatment), polymer dispersions, INS solution (Free-INS) for 120 min (mean values ± SD; n = 3) (B).

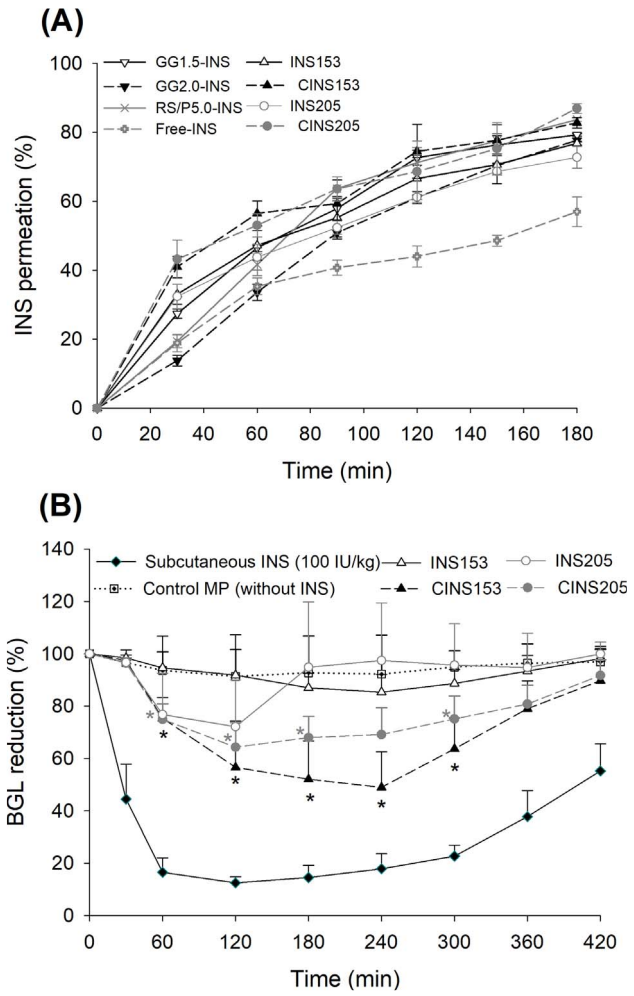

Fig. 5. (A) INS permeation (%) into a tissue chamber from rat colonic sac after introduction of Free-INS, coated (CINS153 and CINS205) and uncoated (INS153 and INS205) MP for 180 min (n = 6) and (B) *In vivo* hypoglycemic effect after oral administration of MP without INS (negative group), coated and uncoated MP containing INS (100 IU/kg) (test group) and subcutaneous injection of INS solution (10 IU/kg) (positive group) on diabetic rats (n = 6). BGL reduction from INS-loaded MP statistically different from unloaded-MP: *$p < .05$.

Table 3
Values of apparent permeability coefficient (P_{app}) of INS and enhancement ratio (R) across Caco-2 monolayers (n = 3) and excised rat intestine (n = 6) (mean values ± SD).

Samples	P_{app} ($\times 10^{-6}$ cm s^{-1})	(R)	P_{app} ($\times 10^{-6}$ cm s^{-1})	(R)
	Caco-2 cell monolayers		Excised rat intestine	
INS153	32.60 ± 1.72	1.39	46.23 ± 1.22	1.80
CINS153	46.45 ± 0.83	1.99	31.45 ± 1.38	1.22
INS205	43.23 ± 3.83	1.85	39.65 ± 4.61	1.54
CINS205	48.08 ± 7.32	2.06	43.52 ± 4.72	1.69
GG1.5-INS	38.52 ± 3.23	1.65	38.19 ± 1.92	1.49
GG2.0-INS	27.29 ± 2.48	1.19	60.60 ± 2.57	2.36
RS/P5.0-INS	50.30 ± 5.97	2.15	186.50 ± 28.16	7.26
Free-INS	23.34 ± 0.09	1.00	25.66 ± 1.49	1.00

(from 42 to 47%), so that the highest transport was from RS/P5.0-INS ($p < .05$), the only dispersion that promoted the TEER reduction.

3.8. Ex vivo INS permeability on intestinal rat tissues

The influence of the microencapsulation and coating processes on INS transport across intestinal epithelium was evaluated using excised intestinal rat tissues (Fig. 5A). On the early stages of the test (until 60 min), the behavior of all samples was quite similar, but over time the permeation of INS carried in MP reached significantly higher values (73–86%) ($p < .05$) than those exhibited by Free-INS (57%). Among the MP, the highest INS transport verified after 180 min of test was from CINS153 and CINS205 possibly due to the action of the RS/P coating on the opening of the TJ as previously demonstrated, therefore optimizing the paracellular transport. Moreover, the combination of RS/P polysaccharides with the GG mucoadhesive polymer probably increased the interaction of MP with the intestinal mucosa, prolonging the contact time with the mucosa and raising the local concentration gradient of the drug, factors that are well established as strategy to enhance permeability [15,61].

Our results show that different concentrations of GG and Al^{3+} used in the preparation of MP did not significantly influence the intestinal permeability ($p > .05$), indicating that the presence of coating was decisive for optimizing the permeation process.

The P_{app} coefficients (Table 3) were significantly increased for MP with absorption enhancement ratio (R) reaching 1.8, demonstrating that INS microencapsulation is quite effective in the improvement of its intestinal permeation. The higher P_{app} and R values for GG2.0-INS and RS/P5.0-INS in relation to those found for MP are probably related to the faster release of INS from these polymeric dispersions, as a result of the less rigid structures that allow the greater INS diffusion. Besides, the high flexibility of their polymer chains also facilitates the interaction with the mucin chains present at mucus layer, increasing the potential

of mucoadhesiveness.

From the analysis of the INS permeation profiles, the non-linear relationship between INS permeated (%) and time (min) is indicative that the INS permeation occurred by both paracellular and transcellular transports [27].

3.9. In vivo hypoglycemic effect on diabetic rats

The efficacy of INS-loaded GG MP coated with RS/P films on reducing glycemia after oral administration was evaluated using alloxan-induced diabetic rats.

The pharmacological response was monitored for 7 h and the reduction of BGL (%) was calculated for each group (Fig. 5B). The blood glucose baseline value (initial glucose level) was taken as 100% and all other blood glucose data were calculated as a percentage of the baseline.

No significant change in glycemia was observed after administration of the MP without INS (negative group). Unlike, the subcutaneous INS injection (positive group) reduced 55.49% of BGL in just 0.5 h, reaching 87.48% in the next 2 h. At the end of the test, the hypoglycemic effect was still quite pronounced (~44.73%).

Orally administered INS-loaded MP showed a significant reduction in glycemia, which occurred gradually, reaching the maximum effect after 2 h for CINS205 (35.70%) and INS205 (27.85%) and after 4 h for samples CINS153 (51.02%) and INS153 (14.65%). The most pronounced hypoglycemic effect for the sample CINS153 (up to 3.5 times highest) can be associated with its greater capacity to permeate the intestinal tissue, together with the greater INS protection against the enzymatic digestion, as earlier demonstrated. Importantly, although glycemia of the rats increased over time, the pharmacological effect of the CINS153 was 10% at the end of the test.

4. Conclusions

Despite of a progressive advance in the development of new drug delivery systems to overcome limited oral bioavailability of insulin, no commercial product is available in the market because of failures in the safeness and effectiveness of such systems, which are mostly nano-scale. We developed a multi-strategy micro-scale technological platform based on natural polysaccharides, using a relatively easier and low cost process. Thanks to this work, it was possible to demonstrate that (i) the coated MP controlled the *in vitro* release of insulin in different pH values, simulating the gastrointestinal tract segments, (ii) the encapsulation promoted a great protection against trypsin and alpha-chymotrypsin degradation during 120 min, (iii) both *ex vivo* and *in vivo* permeation techniques evidenced the enhancement of insulin permeation and (iv) *in vivo* study demonstrated the effective hypoglycemic activity for up to 7 h and the glycemia in diabetic rats could be reduced by up to 51%. Considering that the *in vivo* tests were performed with insulin dosage similar to that used for subcutaneous route, further dosage adjustments for the oral route may allow the significant improvement of the therapeutic effect. The high enzymatic inhibition and increased INS permeability indicate that the polysaccharides employed in this study represent an alternative to the conventional enzyme inhibitors and absorption promoters, respectively, which are often toxic and act in an unspecific way. The set of results demonstrated that the multi-strategy micro-scale technological platform developed in this study represents a promising approach for increasing the oral bioavailability of insulin, collaborating for search by therapeutic alternatives that may make possible the avoiding or reduction of frequency of parenteral administration of INS, providing better quality of life to the patient.

Acknowledgments

The authors are thankful to São Paulo Research Foundation (FAPESP) for providing financial support to accomplish this work (Process n° 2015/01268-2). Moreover, we are grateful to the Research Group CIDAM (conception, engineering and development of food and drug) of the Faculty of Pharmacy of Clermont-Ferrand at Auvergne University in France. We would like to dedicate this work to the memory of our dear Professor Raul Cesar Evangelista.

Declaration of conflicts of interest

The authors report no conflicts of interest associated with this publication.

References

[1] M.C. Koetting, J.F. Guido, M. Gupta, A. Zhang, N.A. Peppas, pH responsive and enzymatically-responsive hydrogel microparticles for the oral delivery of therapeutic proteins: Effects of protein size, crosslinking density, and hydrogel degradation on protein delivery, J. Control. Release 221 (2016) 18–25.
[2] P.J. Carter, Introduction to current and future protein therapeutics: a protein engineering perspective, Exp. Cell. Res. 317 (2011) 1261–1269.
[3] M. Kinch, An overview of FDA-approved biologics medicines, Drug Discov. Today 20 (2015) 393–398.
[4] C.P. Reis, C. Damgé, Nanotechnology as a promising strategy for alternative routes of insulin delivery, in: N. Düzgüneş (Ed.), Methods in Enzymology, Academic Press, Cambridge, 2012, pp. 271–294.
[5] A. Babiker, V. Datta, Lipoatrophy with insulin analogues in type I diabetes, Arch. Dis. Child. 96 (2010) 101–102.
[6] X. Zhang, X. Zhang, Z. Wu, X. Gao, S. Shu, Z. Wang, C. Li, β-Cyclodextrin grafting hyperbranched polyglycerols as carriers for nasal insulin delivery, Carbohydr. Polym. 84 (2011) 1419–1425.
[7] Y. Onuki, M. Morishita, K. Takayama, S. Tokiwa, Y. Chiba, K. Isowa, T. Nagai, *In vivo* effects of highly purified docosahexaenoic acid on rectal insulin absorption, Int. J. Pharm. 198 (2000) 147–156.
[8] S. Chono, R. Fukuchi, T. Seki, K. Morimoto, Aerosolized liposomes with dipalmitoyl phosphatidylcholine enhance pulmonary insulin delivery, J. Control. Release 137 (2009) 104–109.
[9] K.M. Yerramsetty, V.K. Rachakonda, B.J. Neely, S.V. Madihally, K.A.M. Gasem, Effect of different enhancers on the transdermal permeation of insulin analog, Int. J. Pharm. 398 (2010) 83–92.
[10] N.A. Peppas, N.J. Kavimandan, Nanoscale analysis of protein and peptide absorption: insulin absorption using complexation and pH-sensitive hydrogels as delivery vehicles, Eur. J. Pharm. Sci. 29 (2006) 183–197.
[11] O. Pillai, R. Panchagnula, Insulin therapies – past, present and future, Drug Discov. Today. 6 (2001) 1056–1061.
[12] A. Kumar, S.S. Lahiri, H. Singh, Development of PEGDMA: MAA based hydrogel microparticles for oral insulin delivery, Int. J. Pharm. 323 (2006) 117–124.
[13] M.R. Rekha, C.P. Sharma, Oral delivery of therapeutic protein/peptide for diabetes – future perspectives, Int. J. Pharm. 440 (2013) 48–62.
[14] E.S. Khafagy, M. Morishita, Y. Onuki, K. Takayama, Current challenges in non-invasive insulin delivery systems: a comparative review, Adv. Drug Deliv. Rev. 59 (2007) 1521–1546.
[15] N.A. Peppas, Devices based on intelligent biopolymers for oral protein delivery, Int. J. Pharm. 277 (2004) 11–17.
[16] F.G. Prezotti, B.S.F. Cury, R.C. Evangelista, Mucoadhesive beads of gellan gum/pectin intended to controlled delivery of drugs, Carbohydr. Polym. 113 (2014) 286–295.
[17] S. Maiti, S. Ranjit, R. Mondol, S. Ray, B. Sa, Al^{+3} ion cross-linked and acetalated gellan hydrogel network beads for prolonged release of glipizide, Carbohydr. Polym. 85 (2011) 164–172.
[18] H. Hsein, G. Garrait, E. Beyssac, V. Hoffart, Whey protein mucoadhesive properties for oral drug delivery: mucin–whey protein interaction and mucoadhesive bond strength, Colloid. Surface B 136 (2015) 799–808.
[19] M. Narkar, P. Sher, A. Pawar, Stomach-specific controlled release gellan beads of acid-soluble drug prepared by ionotropic gelation method, AAPS PharmSciTech. 11 (2010) 267–277.
[20] B.F. Choonara, Y.E. Choonara, P. Kumar, D. Bijukumar, L.C. du Toit, V. Pillay, A review of advanced oral drug delivery technologies facilitating the protection and absorption of protein and peptide molecules, Biotechnol. Adv. 32 (2014) 1269–1282.
[21] A. Maroni, M.D. Del Curto, S. Salmaso, L. Zema, A. Melocchi, P. Caliceti, A. Gazzaniga, *In vitro* and *in vivo* evaluation of an oral multiple-unit formulation for colonic delivery of insulin, Eur. J. Pharm. Biopharm. 108 (2016) 76–82.
[22] L. Salvioni, L. Fiandra, M.D. Del Curto, S. Mazzucchelli, R. Allevi, M. Truffi, L. Sorrentino, B. Santini, M. Cerea, L. Palugan, F. Corsi, M. Colombo, Oral delivery of insulin via polyethylene imine-based nanoparticles for colonic release allows glycemic control in diabetic rats, Pharmacol. Res. 110 (2016) 122–130.
[23] G. Perera, J. Barthelmes, A. Bernkop-Schnürch, Novel pectin–4-aminothiophenole conjugate microparticles for colon-specific drug delivery, J. Control. Release. 145 (2010) 240–246.
[24] A.B. Meneguin, B.S.F. Cury, R.C. Evangelista, Films from resistant starch-pectin dispersions intended for colonic drug delivery, Carbohydr. Polym. 99 (2014)

140–149.
[25] A.B. Meneguin, B.S.F. Cury, A.M. dos Santos, D.F. Franco, H.S. Barud, E.C. da Silva Filho, Resistant starch/pectin free-standing films reinforced with nanocellulose intended for colonic methotrexate release, Carbohydr. Polym. 157 (2017) 1013–1023.
[26] L.W. Hsu, P.L. Lee, C.T. Chen, F.L. Mi, J.H. Juang, S.M. Hwang, Y.C. Ho, H.W. Sung, Elucidating the signaling mechanism of an epithelial tight-junction opening induced by chitosan, Biomaterial 33 (2012) 6254–6263.
[27] E. Déat-Lainé, V. Hoffart, G. Garrait, E. Beyssac, Whey protein and alginate hydrogel microparticles for insulin intestinal absorption: evaluation of permeability enhancement properties on Caco-2 cells, Int. J. Pharm. 453 (2013) 336–342.
[28] Y. Lv, J. Zhang, Y. Song, B. Wang, S. Wang, S. Zhao, G. Lv, X. Ma, Natural anionic polymer acts as highly efficient trypsin inhibitor based on an electrostatic interaction mechanism, Macromol. Rapid Commun. 35 (2014) 1606–1610.
[29] F. Lacaz-Vieira, Calcium site specificity. Early Ca^{2+}-related tight junction events, J. Gen. Physiol. 110 (1997) 727–740.
[30] S. Sajeesh, K. Bouchemal, V. Marsaud, C. Vauthier, C.P. Sharma, Cyclodextrin complexed insulin encapsulated hydrogel microparticles: an oral delivery system for insulin, J. Control. Release 147 (2010) 377–384.
[31] D. Ameye, J. Voorspoels, J.P. Remon, J. Demeester, S.C. de Smedt, Optimization of an *in vitro* procedure for the determination of the enzymatic inhibition potency of multifunctional polymers, J. Control. Release 68 (2000) 413–417.
[32] H.G.O. Barud, H.S. Barud, M. Cavicchioli, T.S. Amaral, O.B. Oliveira Jr., D.M. Santos, A.L.O.A. Petersen, F. Celes, V.M. Borges, C.O. Oliveira, P.F. Oliveira, R.A. Furtado, D.C. Tavares, S.J.L. Ribeiro, Preparation and characterization of a bacterial cellulose/silk fibroin sponge scaffold for tissue regeneration, Carbohydr. Polym. 128 (2015) 41–51.
[33] C. Ibie, R. Knott, C.J. Thompson, In-vitro evaluation of the effect of polymer structure on uptake of novel polymer-insulin polyelectrolyte complexes by human epithelial cells, Int. J. Pharm. 479 (2015) 103–117.
[34] S. Chakrabortya, S. Janaa, A. Gandhi, K.K. Sena, W. Zhiang, C Gellan Kokare, gum microspheres containing a novel -amylase from marine *Nocardiopsis sp*. strain B2 for immobilization, Int. J. Biol. Macromol. 70 (2014) 292–299.
[35] S. Kanesaka, T. Watanabe, S. Matsukawa, Binding effect of Cu^{2+} as a trigger on the sol-to-gel and the coil-to-helix transition processes of polysaccharide gellan gum, Biomacromolecules 5 (2004) 863–868.
[36] F. Kedzierewicz, C. Lombry, R. Rios, M. Hoffman, P. Maincent, Effect of the formulation on the *in vitro* release of propranolol from gellan beads, Int. J. Pharm. 178 (1999) 129–136.
[37] E.S. Chan, B.B. Lee, P. Ravindra, D. Poncelet, Prediction models for shape and size of ca-alginate macrobeads produced through extrusion–dripping method, J. Colloid Interface Sci. 338 (2009) 63–72.
[38] S.S. Bhattacharya, S. Banerjee, A.K. Ghosh, P. Chattopadhyay, A. Verma, A. Ghosh, A RP-HPLC method for quantification of diclofenac sodium released from biological macromolecules, Int. J. Biol. Macromol. 58 (2013) 354–359.
[39] R.J. Babu, S. Sathigari, M.T. Kumar, J.K. Pandit, Formulation of controlled release gellan gum macro beads of amoxicillin, Curr. Drug Deliv. 7 (2010) 36–43.
[40] E.A. Hosny, A.A.-R. Al-Helw, Effect of coating of aluminium carboxymethylcellulose beads on the release and bioavailability of diclofenac sodium, Pharm. Acta Helvetiae 72 (1998) 255–261.
[41] A.K. Nayak, B. Das, R. Maji, Calcium alginate/gum arabic beads containing glibenclamide: development and in vitro characterization, Int. J. Biol. Macromol. 51 (2012) 1070–1078.
[42] T. Reddy, S. Tammishetti, Gastric resistant microbeads of metal ion cross-linked carboxymethyl guar gum for oral drug delivery, J. Microencapsul. 19 (2002) 311–318.
[43] Y. Zhang, W. Wei, P. Lv, L. Wang, G. Ma, Preparation and evaluation of alginate–chitosan microspheres for oral delivery of insulin, Eur. J. Pharm. Biopharm. 77 (2011) 11–19.
[44] D. Tahtat, M. Mahlous, S. Benamer, A.N. Khodja, H. Oussedik-Oumedhi, F. Laraba-Djebari, Oral delivery of insulin from alginate/chitosan crosslinked by glutaraldehyde, Int. J. Biol. Macromol. 58 (2013) 160–168.
[45] S. Sajeesh, C.P. Sharma, Mucoadhesive hydrogel microparticles based on poly (methacrylic acid-vinyl pyrrolidone)-chitosan for oral drug delivery, Drug Deliv. 18 (2011) 227–235.
[46] A. Bernkop-Schnurch, The use of inhibitory agents to overcome the enzymatic barrier to perorally administered therapeutic peptides and proteins, J. Control. Release 52 (1998) 1–16.
[47] E. Déat-Lainé, V. Hoffart, J.M. Cardot, M. Subirade, E. Beyssac, Development and *in vitro* characterization of insulin loaded whey protein and alginate microparticles, Int. J. Pharm. 439 (2012) 136–144.
[48] M. Eguchi, T. Ooya, N. Yui, Controlling the mechanism of trypsin inhibition by the numbers of α-cyclodextrins and carboxyl groups in carboxyethylester-poly-rotaxanes, J. Control. Release 96 (2004) 301–307.
[49] P.C. Ferrari, F.M. Souza, L. Giorgetti, G.F. Oliveira, H.G. Ferraz, M.V. Chaud, R.C. Evangelista, Development and *in vitro* evaluation of coated pellets containing chitosan to potential colonic drug delivery, Carbohydr. Polym. 91 (2013) 244–252.
[50] J. Mulhbacher, P. Ispas-Szabo, M.A. Mateescu, Cross-linked high amylose starch derivatives for drug release: II. swelling properties and mechanistic study, Int. J. Pharm. 278 (2004) 231–238.
[51] A.K. Nayak, D. Pal, K. Santra, Ispaghula mucilage-gellan mucoadhesive beads of metformin HCl: development by response surface methodology, Carbohydr. Polym. 107 (2014) 41–50.
[52] A. Dimantov, E. Kesselman, E. Shimoni, Surface characterization and dissolution properties of high amylose corn starch–pectin coatings, Food Hydrocolloid 18 (2004) 29–37.
[53] B.S.F. Cury, A.B. Meneguin, V.M.O. Cardoso, F.G. Prezotti, Oral drug release systems based on pectin, in: P.L. Bush (Ed.), Pectin: Chemical Properties, Uses and Health Benefits, Nova Science Publishers, New York, 2014, pp. 65–81.
[54] R.W. Korsmeyer, R. Gurny, E. Doelker, P. Buri, N.A. Peppas, Mechanisms of solute release from porous hydrophilic polymers, Int. J. Pharm. 15 (1983) 25–35.
[55] S.M. Van der Merwe, J.C. Verhoef, J.H.M. Verheijden, A.F. Kotzé, H.E. Junginger, Trimethylated chitosan as polymeric absorption enhancer for improved peroral delivery of peptide drugs, Eur. J. Pharm. Biopharm. 58 (2004) 225–235.
[56] C. Hilgendorf, H. Spahn-Langguth, C.G. Regårdh, E. Lipka, G.L. Amidon, P. Langguth, Caco-2 versus caco-2/HT29-MTX co-cultured cell lines: permeabilities via diffusion, inside- and outside-directed carrier-mediated transport, J. Pharm. Sci. 89 (2000) 63–75.
[57] G. Sandri, M.C. Bonferoni, S. Rossi, F. Ferrari, C. Boselli, C. Caramella, Insulin loaded nanoparticles based on N-trimethyl chitosan: *in vitro* (caco-2 model) and *ex vivo* (excised rat jejunum, duodenum, and ileum) evaluation of penetration enhancement properties, AAPS Pharm. Sci. Tech. 11 (2010) 362–371.
[58] J. Kowapradit, P. Opanasopit, T. Ngawhirunpat, T. Rojanarata, W. Sajomsang, Structure–activity relationships of methylated N-aryl chitosan derivatives for enhancing paracellular permeability across Caco-2 cells, Carbohydr. Polym. 83 (2011) 430–437.
[59] N. Salamat-Miller, T.P. Johnston, Current strategies used to enhance the paracellular transport of therapeutic polypeptides across the intestinal epithelium, Int. J. Pharm. 294 (2005) 201–216.
[60] M. Nur, T. Vasiljevic, Can natural polymers assist in delivering insulin orally? Int. J. Biol. Macromol. 103 (October 2017) 889–901.
[61] G.P. Andrews, T.P. Laverty, D.S. Jones, Mucoadhesive polymeric platforms for controlled drug delivery, Eur. J. Pharm. Biopharm. 71 (2009) 505–518.